6th Australasian Hydraulics and
Fluid Mechanics Conference
Adelaide, Australia, 5-9 December 1977

Cross-Flow Characteristics on a Cylindrical Body at Incidence in Subsonic Flow

M. L. ROBINSON
Senior Research Scientist, Aerospace Division, Weapons Research Establishment

SUMMARY The flow over a cylindrical body at incidence is examined with special reference to the behaviour and role of the attachment line boundary layer. Results of previous work on the flow on the leading edges of swept wings are used to establish conditions governing cross-flow behaviour on an inclined cylinder. Flow observations and measurements of forces and moments on a cylindrical body have confirmed the theoretical prediction that, over a range of Reynolds number encountered in wind tunnel testing, an initially turbulent cross-flow reverts to a predominantly laminar flow at a critical incidence angle. Both Reynolds number and conditions on the nose such as roughness greatly influence the critical incidence angle.

1 INTRODUCTION

At low angles of inclination the potential flow over a streamlined body of revolution is insensitive to viscous effects since the boundary layer displacement thickness is only weakly dependent on Reynolds number, and changes in effective body contour are then relatively small. At moderate incidence angles at which a substantial velocity component exists normal to the axis of the body, viscous effects exert a large influence on the flow because the cross-flow characteristics are sensitive to the state of the cross-flow boundary layer.

The impulse flow analogy in which the cross-flow on a body at incidence is related to the flow over an impulsively started cylinder has been used as the basis of methods (Thomson, 1972) for predicting the viscous forces and moments acting on an inclined body. Whereas the available methods give satisfactory estimates of the forces and moments acting on inclined bodies of revolution up to incidence angles of about 15°, there is a need to consider more closely the mechanics of the boundary layer in the mixed axial-/cross-flow situation on the body. It is the purpose of this paper to reconcile the nature of the cross-flow and the resulting forces and moments with the state of the boundary layer on the attachment line of the body. This boundary layer is sensitive to disturbances originating on the nose which amplify, decay or remain neutrally stable according to the momentum thickness Reynolds number of the attachment line boundary layer.

2 FLOW DESCRIPTION

In the flow over a body at and near zero incidence, the streamwise velocity component dominates the flow, and the location of transition is then determined by known quantities such as Reynolds number based on a reference length, Mach number, freestream turbulence, pressure gradients on the nose, roughness and heat transfer. As incidence is increased, a normal velocity component is superimposed on the axial component, and a recognizable cross-flow becomes established. Attributes of the typical cross-flow are a well-defined attachment line flow and the onset of flow separation in the cross-flow plane, usually characterized by the formation of two or more streamwise vortices. It is the state of the attachment line boundary layer, whether laminar, transitional or turbulent, which is a crucial element in determining the characteristics of the overall cross-flow pattern.

Except in the vicinity of the nose, the flow on the attachment line of an inclined body is analogous to the corresponding flow on a swept wing with a leading edge of constant radius, where the angle of incidence α of the body is equivalent to the complement of the wing sweep-back angle. Although the three-dimensional flow field on the nose of the body will influence the attachment line boundary layer through the imposed pressure gradient and streamline divergence, this is unlikely to invalidate the general application of the swept wing results to the inclined body. Studies of boundary layer behaviour on the leading edges of swept wings have been carried out by Gaster (1965) and Cumpsty and Head (1969), and the relevant findings of these investigations are outlined in the following paragraphs.

It has been found that the quantity that characterizes the attachment line boundary layer is the Reynolds number based on the momentum thickness θ of the boundary layer on the attachment line, where

$$\theta = 0.404\ (\nu/u_c')^{\frac{1}{2}}$$

for a laminar layer and u_c' is the velocity gradient of the component of the potential flow normal to the axis of the inclined body. The momentum thickness Reynolds number is then given by

$$R_\theta = U_s\theta/\nu = 0.404U_s/(\nu u_c')^{\frac{1}{2}},$$

where U_s is the spanwise velocity component. The velocity gradient u_c' on a circular cylinder can be expressed in terms of cross-flow velocity U_c and body radius r by $u_c' = 2U_c/r$, from which

$$R_\theta = 0.286U_s/(\nu U_c/r)^{\frac{1}{2}}.$$

For present purposes R_θ may be expressed in terms of freestream Reynolds number based on diameter, R_d and incidence α, as follows:

$$R_\theta = 0.20\ (R_d)^{\frac{1}{2}} \cot\alpha\ (\sin\alpha)^{\frac{1}{2}}. \qquad (1)$$

An important result obtained by both Gaster and Cumpsty and Head is that to produce a turbulent

flow on the attachment line of a swept wing, there must be sufficient initial disturbance level in the boundary layer and the momentum thickness Reynolds number must be large enough to sustain turbulence. Under these conditions the flow a long way downstream from the disturbance is fully turbulent and independent of the nature of the disturbance.

With large upstream disturbances, turbulent spots exists, showing no sign of decay for R_θ values as low as 100. The value of R_θ must be not less than 140, however, before the flow has the properties of a turbulent flow corresponding to much higher values of R_θ. The existence of a minimum size of disturbance to induce transition has been verified in the range of R_θ investigated. At large values of R_θ the observations suggest that even for a tripping device only just smaller than the critical size, the flow reverts to a laminar condition, whereas for a tripping device just above the critical size there appears to be immediate transition to a fully turbulent flow.

The momentum thickness Reynolds number computed from equation 1 for a laminar boundary layer on an inclined cylinder is shown in figure 1 as a function of Reynolds number R_d and incidence α. Accepting the notion that the attachment line boundary layer is essentially laminar for momentum thickness Reynolds number less than a critical value (approximately 100 in swept wing tests), then reference to figure 1 shows that for each value of Reynolds number R_d, there exists a maximum angle of incidence beyond which turbulent flow cannot persist on the attachment line.

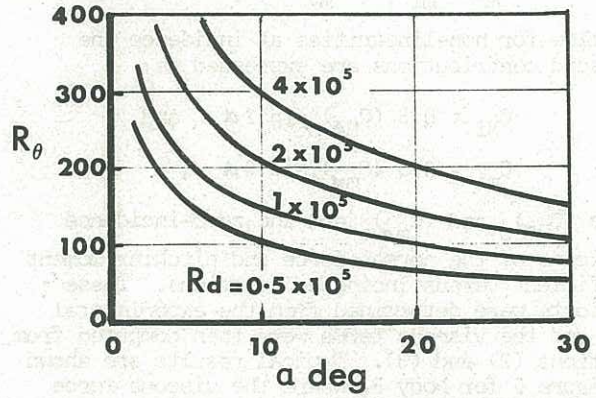

Figure 1 Momentum thickness Reynolds number

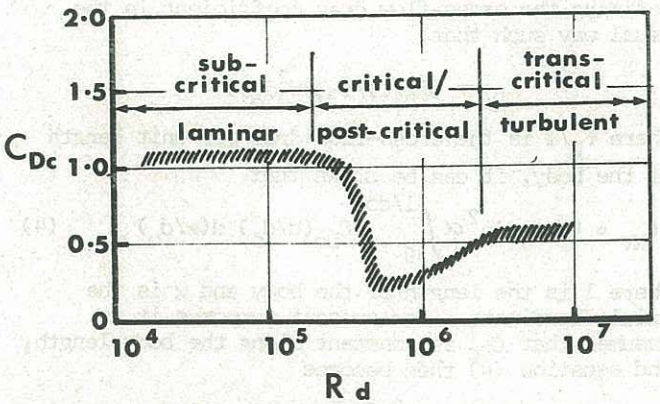

Figure 2 Drag coefficient of two-dimensional cylinder

Since the boundary layer on the attachment line directly influences the total cross-flow, it becomes evident that the flow over the inclined cylinder involves a complex interplay of boundary layer mechanisms. The various cross-flow regimes can be identified by reference to the drag coefficient of a two-dimensional cylinder which is shown in figure 2 for incompressible flow. A wide range of drag coefficient is possible depending on the state of the boundary layer.

In addition to the role of the axial flow along the attachment line in determining the flow over the body, it is reasonable to expect that other axial contamination mechanisms exists, particularly in the separated flow region. To verify the existence of the types of flow described in this section and to obtain the effect of these flows on the forces and moments acting on a cylindrical body, wind tunnel experiments have been carried out and are described in the following section.

3 WIND TUNNEL INVESTIGATION

3.1 Smoke Flow Visualization

Flow visualization studies were made on the test body shown in figure 3 using kerosene smoke injected through a hole in the nose. Stroboscopic lighting was used to illuminate the smoke in the tests which were carried out at a Reynolds number R_d of 6×10^4. A transition ring 0.4 mm in height was used to fix transition on the nose of the body. The flow at inclinations of less than 10° is shown in figure 4(a). The attachment line boundary layer was turbulent downstream of the transition ring and the cross-flow was characteristically turbulent. Downstream of the zone of influence of the nose, the separation line was nearly parallel to the axis of the body and the angle from the attachment line at which separation occurred was about 130°.

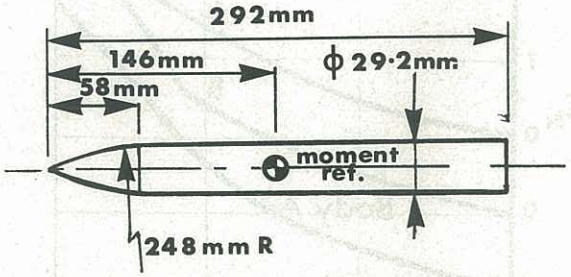

Figure 3 Body geometry

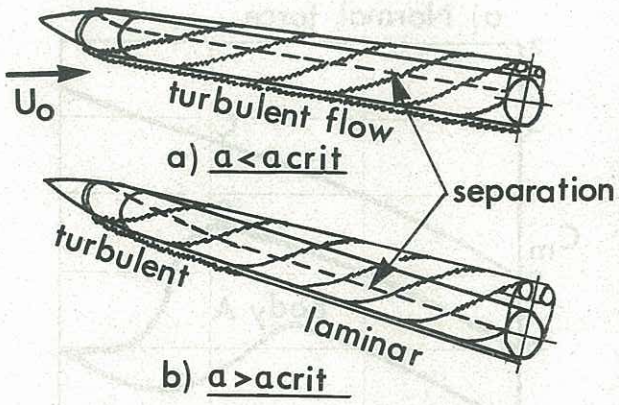

Figure 4 Flow patterns on inclined body

For inclinations in excess of about 12°, laminarization of the attachment line boundary layer occurred with the extent of turbulent flow shrinking towards the nose with increasing incidence. The observed flow is shown in figure 4(b). The cross-flow character was turbulent over the forward portion of the body and laminar over the rearward

portion. Considerable turbulence was evident in the separated shear layers and vortices along the length of body, and it appeared that turbulence convected into the wake near the nose of the body contaminated the entire separated flow field. The angle from the attachment line at which cross-flow separation occurred varied from about 140^{o} near the nose to 90^{o} at the base of the body. In terms of the flow over a two-dimensional cylinder, these values are typical of turbulent and laminar separations respectively.

In these tests the momentum thickness Reynolds number R_θ at an incidence of 10^{o} was 115 from figure 1. This result correlates well with the minimum predicted R_θ value of 100 for which turbulent attachment line flow can be maintained with large disturbances.

4.2 Force Measurement

Force measurement tests were made on the basic body shown in figure 3 at a Mach number of 0.5 and a Reynolds number R_d of 2×10^5. Data were obtained on three versions of the body, namely:
(a) the smooth-nosed body (designated A),
(b) the body with a circumferential row of 0.35 mm dia spheres attached to the nose 30 mm from the tip (B), and
(c) the body with a transition ring 0.2 mm in height located 58 mm from the nose tip (C).
At zero incidence transition occurred in the vicinity of the nose shoulder of body A and at the transition bands of bodies B and C.

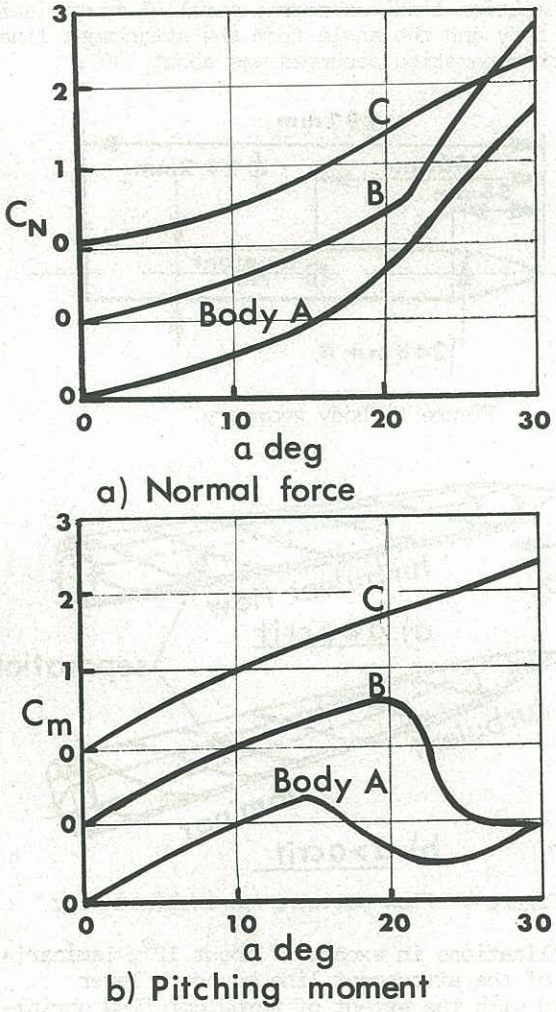

Figure 5 Normal force and pitching moment coefficients

Normal force coefficient C_N and pitching moment coefficient C_m about the mid-point of the body are shown in figure 5 for the bodies A, B and C. By definition,

$$C_N = \text{normal force}/qS \quad \text{and}$$

$$C_m = \text{pitching moment}/qSd_o ,$$

where q is the free-stream dynamic pressure ($\frac{1}{2}\rho U_o^2$), d_o is the cylindrical body diameter and S is the cross-sectional area ($\pi d_o^2/4$). The results show a clearly defined break in the trend of the normal force and pitching moment coefficients as functions of incidence for bodies A and B. This break occurs at an incidence of 14^{o} for body A and 20^{o} for body B, corresponding to R_θ values of 175 and 145. There is no evidence of a similar break in the results for body C in the incidence range 0^{o} to 30^{o}.

It can be inferred that at the observed break or critical incidence incipient laminarization of the flow occurs, and this view is supported by schlieren observations which show a distinct change in vortex pattern at this incidence. However, further analysis of the experimental results is necessary to confirm this hypothesis.

4 RESULTS ANALYSIS

The total normal force and pitching moment coefficients are assumed to be the sum of the inviscid (potential) and viscous contributions as follows:

$$C_N = C_{Ni} + C_{Nv} \quad \text{and} \qquad (2)$$

$$C_m = C_{mi} + C_{mv} . \qquad (3)$$

To allow for non-linearities at incidence the inviscid contributions are expressed as

$$C_{Ni} = 0.5\,(C_{N\alpha})_o \sin 2\alpha \quad \text{and}$$

$$C_{mi} = 0.5\,(C_{m\alpha})_o \sin 2\alpha ,$$

where $(C_{N\alpha})_o$ and $(C_{m\alpha})_o$ are the zero-incidence gradients of the normal force and pitching moment coefficient versus incidence functions. These gradients were determined from the experimental data and the viscous terms were then computed from equations (2) and (3). Typical results are shown in figure 6 for body B, where the viscous force and moment components exhibit the marked change in trend with incidence at 20^{o}.

Defining the cross-flow drag coefficient in the usual way such that,

$$C_{Dc} = (F_D/l)/(\tfrac{1}{2}\rho U_c^2 d_o),$$

where F_D/l is the cross-flow drag per unit length of the body, it can be shown that

$$C_{Nv} = 4/\pi \sin^2\alpha \int_0^{l/do} C_{Dc}(d/d_o)\, d(x/d_o) , \qquad (4)$$

where l is the length of the body and x is the axial coordinate. For present purposes it is assumed that C_{Dc} is constant along the body length, and equation (4) then becomes

$$C_{Nv} = 4/\pi \sin^2\alpha \; 9.17\, C_{Dc} . \qquad (5)$$

The cross-flow drag coefficient computed from equation (5) is shown in figure 7 for bodies A, B and C.

Below the critical incidence, the derived mean

values of C_{Dc} lie between 0.32 and 0.52, and above the critical incidence C_{Dc} gradually increases to about 1.0 for bodies A and B at $\alpha = 30^{\circ}$. Using data from Hoerner (1965), the above values have been corrected for the effect of finite length to diameter ratio to yield equivalent two-dimensional drag coefficients between 0.45 and 0.73 below the critical incidence, increasing to 1.4 at $\alpha = 30^{\circ}$. Drag coefficients of 0.5 to 0.7 are typical of turbulent transcritical flow on a smooth cylinder (Jones, Cincotta and Walker, 1969), whereas a drag coefficient of 1.4 corresponds to laminar subcritical flow (Thomson, 1972). The drag coefficient of about 0.45 obtained on body A may correspond to a post-critical cross-flow condition, in which turbulent reattachment and separation follow a laminar separation bubble. Even though R_θ exceeded 175 below the critical incidence, the low disturbance level in the boundary layer on the smooth nose may have been insufficient to induce turbulence on the attachment line.

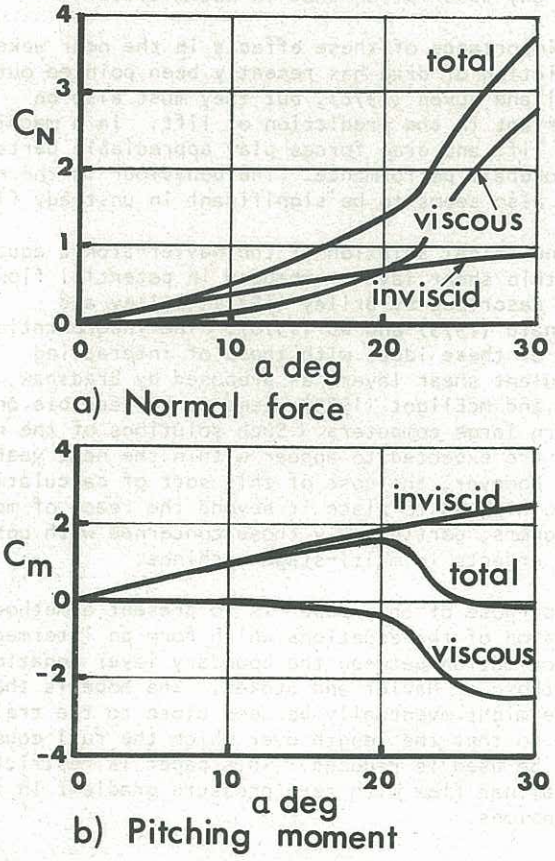

Figure 6 Normal force and pitching moment components - body B

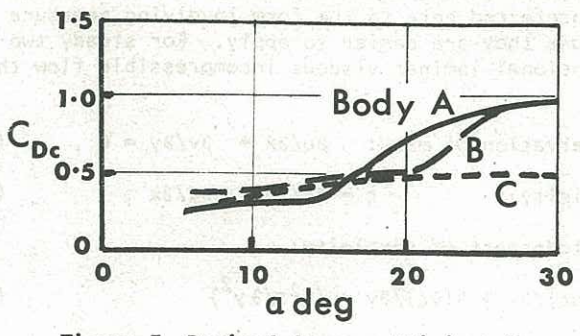

Figure 7 Derived drag coefficient C_{Dc}

It is noteworthy that the cross-flow drag coefficient of body C with the 0.2 mm high transition band on the nose shoulder corresponds to turbulent cross-flow throughout the present incidence range. At 30° incidence, R_θ reaches a minimum value of 110 which just exceeds the value of 100 at which the appearance of turbulent flow can be maintained on the attachment line with a very high level of disturbance in the boundary layer.

If the cross-flow drag was uniformly distributed along the length of the body, the centre of pressure position of the viscous normal force would be located 5.4 calibre from the nose. The results show that the centre of pressure positions corresponding to turbulent cross-flow are in fact situated within about 0.5 calibre of this position for incidence angles greater than 10°. As flow laminarization first occurs, the centre of pressure position initially moves rearwards by between 0.6 and 0.8 calibre.

Summing up, the experimental evidence fully supports the proposition that the attachment line boundary layer is the key factor in determining the nature of the cross-flow on an inclined cylindrical body. As in the swept wing experiments, the nature of the attachment line boundary layer has been found to depend primarily on the momentum thickness Reynolds number R_θ and the disturbance level in the boundary layer on the nose.

5 CONCLUSIONS

On the basis of flow observations and force measurements, it is clear that at least two distinct flows are possible on a body at a Reynolds number R_d of 2×10^5. A critical incidence angle exists below which the total flow on the body is either fully turbulent or turbulent at separation, and above which laminarization of the flow takes place. An equivalent two-dimensional drag coefficient of 0.6 is appropriate for turbulent cross-flow and 1.4 for the laminar case. The centre of pressure of the turbulent cross-flow normal force is situated close to the centroid of the planform of the body.

The critical incidence corresponds to an R_θ value varying from 175 for the smooth-nosed body with natural transition down to less than 110 for body C with a transition band. Relaminarization of the flow above the critical incidence takes place over a range of R_θ and hence incidence, depending on conditions on the nose.

6 REFERENCES

THOMSON, K.D. (1972). The estimation of viscous normal force, pitching moment, side force and yawing moment on bodies of revolution at incidences up to 90°. WRE-Report-782 (WR&D).

GASTER, M. (1965). On the flow along swept leading edges. College of Aeronautics Note Aero 167.

CUMPSTY, N.A. and HEAD, M.R. (1969). The calculation of the three-dimensional boundary layer. The Aeronautical Quarterly, Vol. 20, pp 99-113.

HOERNER, S.F. (1965). Fluid-dynamic drag. New Jersey, Published by the author.

JONES, G.W., CINCOTTA, J.J. and WALKER, R.W. (1969) Aerodynamic forces on a stationary and oscillating circular cylinder at high Reynolds numbers. NASA TR R-300.